Journal of Alloys and Compounds 509 (2011) 4348–4351

Contents lists available at ScienceDirect

Journal of Alloys and Compounds

journal homepage: www.elsevier.com/locate/jallcom

Y_2O_3–BaO–SiO_2–B_2O_3–Al_2O_3 glass sealant for solid oxide fuel cells

Shouguo Huang*, Qiliang Lu, Chunchang Wang*

Laboratory for Dielectric Functional Materials, School of Physics and Materials Science, Anhui University, Hefei 230039, PR China

ARTICLE INFO

Article history:
Received 6 December 2010
Received in revised form 7 January 2011
Accepted 7 January 2011
Available online 14 January 2011

Keywords:
Fuel cells
Thermal expansion
Glass
Sealant

ABSTRACT

A glass based on Y_2O_3–BaO–SiO_2–B_2O_3–Al_2O_3 (named YBA) has been investigated as sealant for planar solid oxide fuel cells (SOFCs). The YBA glass has been systematically characterized by differential thermal analysis, dilatometer, scanning electron microscopy, impedance analysis, and open circuit voltage to examine their suitability as sealant. The coefficient of thermal expansion of YBA is $11.64 \times 10^{-6}\,K^{-1}$ between 323 and 873 K. The resistivity is $9.1 \times 10^4\,\Omega$ cm at 800 °C. The glass sealant is found to be well adhered with other cell components, such as electrolytes and stainless steels, at an optimum sealing temperature of 800 °C. All measured results showed that the YBA glass appears to be a promising sealant for SOFCs.

1. Introduction

Solid oxide fuel cells (SOFCs) convert chemical energy direct into electric energy with high-energy conversion efficiency and low emissions. Generally, there are two basic designs for the SOFC stacks: tubular and planar. Planar SOFCs have become increasingly attractive, since planar SOFCs can potentially offer lower cost and higher power density per unit volume compared with tubular designs [1–3]. However, it is necessary to develop a suitable sealant for planar SOFCs, which can prevent the fuel gas and air from mixing during fuel cell operation, and insulate the stack to the atmosphere [4,5]. Thus, to develop such gas-tight and durable sealant is one of the major technological challenges for the planar SOFC stack developers.

The sealants for planar SOFCs must meet the following requirements: (a) matching coefficient of thermal expansion (CTE) with other SOFC components; (b) good bonding property to the fuel cell components; (c) high electrical resistivity to avoid short-circuiting between different layers of the stack (>2 kΩ cm); (d) good thermochemical compatibility with relevant SOFC components (that is, no harmful reaction with joining components); and high chemical stability and low vapor pressure in both reducing and oxidizing atmospheres; (e) nonspreading to the adjoining fuel cell components at the operating temperature; (f) deformability but must be able to withstand a slight overpressure. Also the mechanical strength of the stack has to be guaranteed.

In general, glass or glass–ceramic sealants can meet almost all the above-mentioned requirements. The remarkable advantage of these sealants is the chemical compositions of the glass that can be tailored to optimize some important physical properties such as matching CTE, appropriate viscosity. So far, most SOFC sealant development has focused on glass or glass–ceramic sealants, although other approaches, such as cement sealants, mica glass–ceramics, brazes and compressive seals, have been proposed [6–14].

To develop a suitable glass sealant for planar SOFCs, many studies have been carried out with the purpose of the applications of the glass or glass–ceramic-based materials like alkali silicate, alkaline-earth silicate, alkali borosilicate such as Pyrex,n aluminophosphate [15–27]. However, each material has a few drawbacks known as high thermal mismatch, and poor long-term stability due to the active interface reaction with other SOFC components.

The present study aimed at developing suitable glass sealants of Y_2O_3–BaO–SiO_2–B_2O_3–Al_2O_3 for planar SOFCs at relatively lower sealing temperature (~800 °C), especially suitable for anode-supported planar SOFCs operating between 750 °C and 800 °C. To estimate the applicability of these glasses as sealants, their thermal properties, viscosity, microstructure, conductivity, and the overall bonding characteristics were examined.

2. Experimental

The YBA glass was made from reagent-grade $BaCO_3$, Al_2O_3, Y_2O_3, B_2O_3 and SiO_2. The detailed chemical composition of the YBA glass is given in Table 1. The thoroughly mixed batch was melted in an electric furnace at 1200 °C for 4 h using a Pt–Rd 10% crucible, and poured into a steel mold to produce bulk glasses that were subsequently annealed at a temperature around 550 °C. Then, the bulk glasses were cut into bar-typed specimen (20 mm in length) for CTE measurements, or milled into fine powders (30–40 μm) for fabricating pressed bar-typed specimen or glass pellets.

* Corresponding authors. Tel.: +86 551 5107284; fax: +86 551 5846849.
E-mail addresses: huangsg@ustc.edu (S. Huang), ccwang@ahu.edu.cn (C. Wang).

0925-8388/$ – see front matter © 2011 Elsevier B.V. All rights reserved.
doi:10.1016/j.jallcom.2011.01.070

Table 1
Component ration of the YBA glass (wt.%) in this work.

Y_2O_3	BaO	Al_2O_3	SiO_2	B_2O_3
10	60	7.21	3.53	19.26

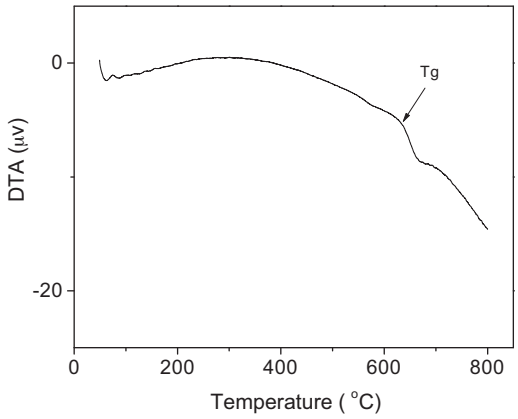

Fig. 1. DTA plot of the YBA glass.

Detailed DTA studies were carried out using a thermal analyzer (Netzsch STA 429). The glass transition temperature obtained from DTA was compared with the softening temperature resulting from a thermomechanical analyzer (Netzsch DIL 402C). The CTE values were obtained using a dilatometer (Netzsch DIL 402C) performed in air with a heating rate of 5 K/min.

The microstructures between the glass and the SOFC components were analyzed by a scanning electron microscopy (SEM, Hitachi 650).The conductivity of the YBA glass at different temperatures were detected using an electrochemical impedance spectroscopy (CHENHUA, CHI 604A).

The sealing test of the YBA glass was carried out by measuring the open circuit voltage of a cell at 750 °C. The cell was fabricated using an yttrium-stabilized zirconium (8 mol%,YSZ,) pellet (ϕ15 mm, sintering at 1400 °C for 4 h), and printed with silver paste on both sides. The pure hydrogen and air were used as the fuel and oxidant gas, respectively.

3. Results and discussion

Fig. 1 shows the DTA plot of the YBA glass. The endothermic peak between the temperature range 893 and 903 K is due to the glass transition. The transition temperature, T_g of the YBA glass lies within the temperature range 893–903 K, which is below the SOFC operating temperature. No phase transformation occurs at lower or higher temperatures.

In order to enable thermal cycling of the stacks, the CTE mismatch of the different materials has to be as small as possible. Fig. 2 shows the linear thermal expansion curve of the YBA glass. The sealant expands linearly in the temperature range 323–873 K, and the CTE is found to be $11.64 \times 10^{-6}\,K^{-1}$, which is close to those of other SOFC components, for example, CTE of YSZ or SDC (samaria-doped cerium) is about $10.2–12.8 \times 10^{-6}\,K^{-1}$. The slope of the curve between T_g and T_s (soft temperature) shows a dramatic increase in expansion just before the viscous flow makes the glass to deform. However, the curve inflects upward over 898 K and drops down at 948 K. This phenomenon is related to the transformation of glass and the following calculations are based on the analysis of this curve. The sealant becomes soft and flexible over 898 K, thus it is easy to match with other adjacent components. It should be noted that the difference in CTE between the glass and other components is less than 10%. The stress arising from the CTE mismatch can be tolerated by the sealant at the cell operating temperature where the stress is being released by viscous flow.

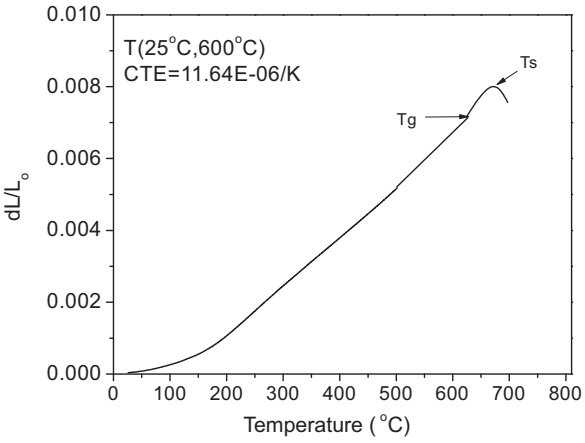

Fig. 2. CTE plot of the YBA glass.

The T_s obtained from the thermal expansion curve, was found to be 948 K as the CTE reaches a maximum value. By fitting the two linear parts of the thermal expansion curve, the T_g can be obtained, and the value is 898 K. The sealant for SOFCs has to be stronger and stiffer in order to achieve mechanically stable stacks that can be handled and withstand pressure differences during operation. On the other hand, the sealant must be soft enough to reduce mechanical stresses occurring during production and in operation.

From Figs. 1 and 2, the T_g and T_s were deduced as 898 K and 948 K. According to the simple liquid theory (Mott and Gurney) and Beaman results, there is a relationship between the melting point (T_m) and T_g [28]:

$$\frac{T_g}{T_m} = \frac{2}{3} \tag{1}$$

So, T_m can be calculated as T_m = 1247 K.

The sealant viscosity decides the sealing (joining) and operating temperatures. The glass viscosities at different temperatures can be calculated by the Vogel–Fulcher–Tammann (VFT) equation [29]:

$$\log \eta = \frac{A + B}{(T - T_0)} \tag{2}$$

where A, B and T_0 are constants.

The typical viscosity values of the YBA glass at the corresponding temperatures are given in Table 2. Thus, the relationship of viscosity

Table 2
The typical viscosity values of the YBA glass at the corresponding temperatures.

T (K)	898	948	1247
η (Pa s)	$10^{12.4}$	10^{8}	10^{5}

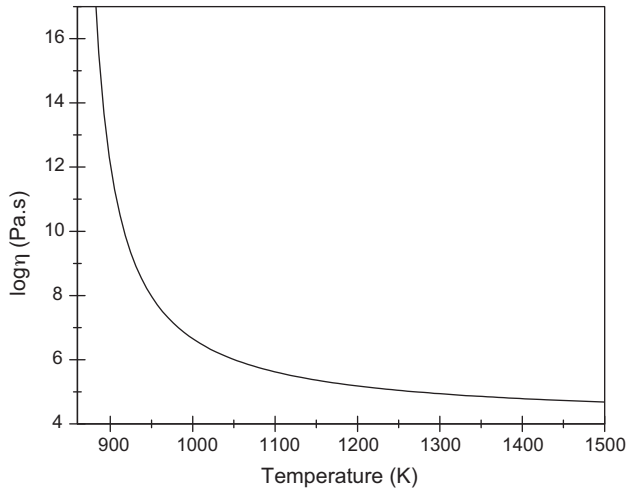

Fig. 3. Viscosity–temperature curve of the YBA glass.

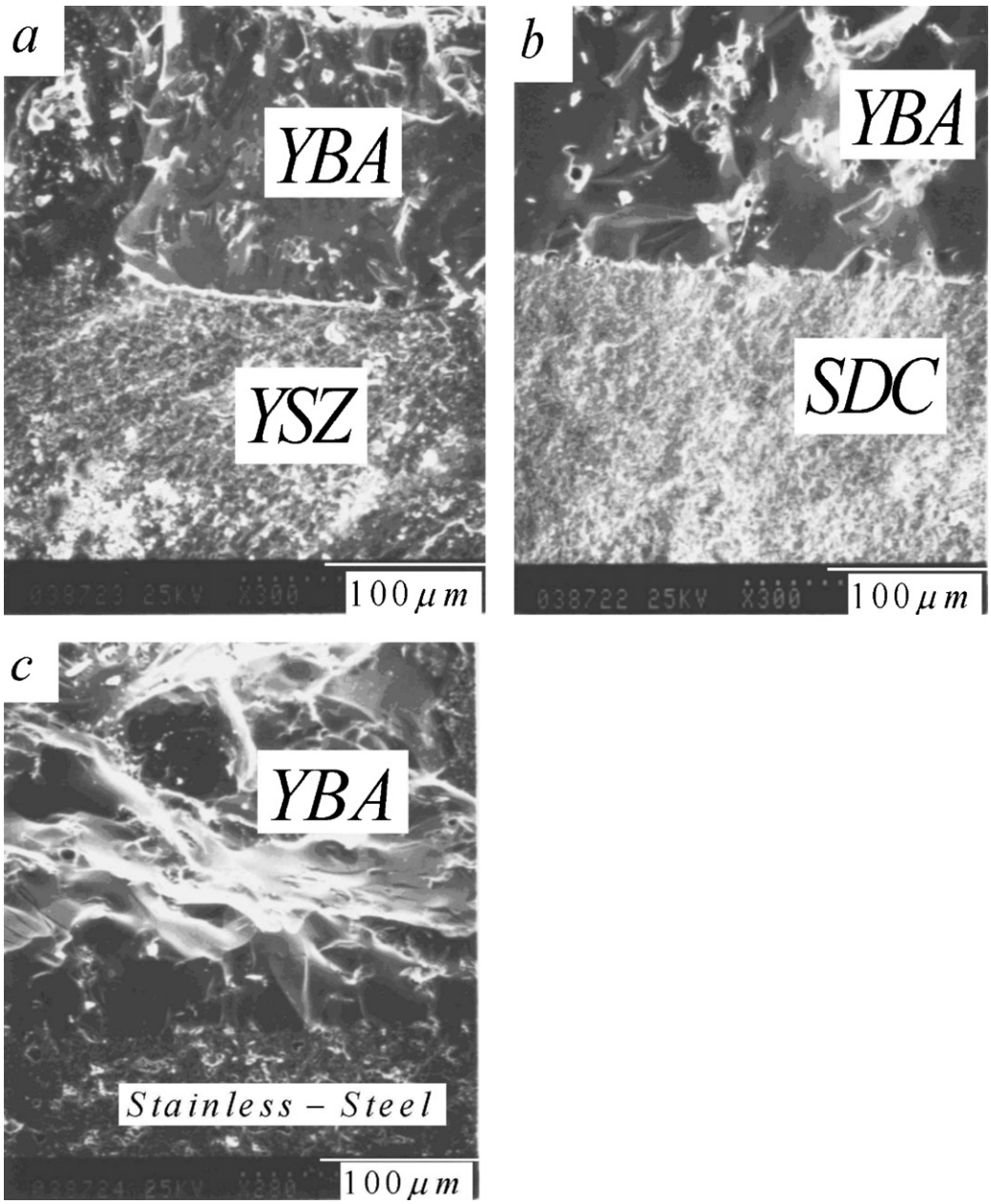

Fig. 4. SEM images of the interfaces between the YBA glass and (a) YSZ, (b) SDC, and (c) stainless steel.

and temperature can be written as:

$$\log \eta = \frac{4.1 + 375.2}{(T - 853.1)} \tag{3}$$

The viscosity–temperature curve of the YBA glass has been shown in Fig. 3. The viscosity value as determined at the sealing temperature (800 °C) is ~105.81 Pa s, which is very desirable for sealing applications that required a viscosity value typically of 105–108 Pa s.

Fig. 4 shows the microstructures of the YBA glass/YSZ (SDC, stainless steel) interfaces after being bonded at 800 °C for 30 min. One can see that the glass adhered on YSZ (SDC, stainless steel) very well. It is apparent not only the glass is completely bonded with them without cracks, but also that no reaction product layer is formed. Although a relatively dense glass was achieved, there are still existing some closed pores in the glass region. It needs higher sealing temperature or longer sealing time to remove those pores. Details about this feature as well as the interface reaction and diffusion of elements between glass and other cell components await further investigation.

Fig. 5 shows the Arrhenius plot of the electrical conductivity of the YBA glass. One can see the resistivity decreases with increasing temperature like most other glasses. The decrease in resistivity values with increasing temperature might be due to ionic conductivity associated with the migration of Ba ions. The resistivity of the YBA glass at 800 °C is $9.1 \times 10^4\ \Omega$ cm. The resistivity is high enough in the temperature range from 700 to 800 °C for the application of SOFCs.

A linear plot of $\mathrm{Ln}(\sigma T)$ versus $1/T$ confirms the Arrhenius behavior which is governed by the following well known equation:

$$\sigma T = A \exp\left(\frac{-E_a}{kT}\right) \tag{4}$$

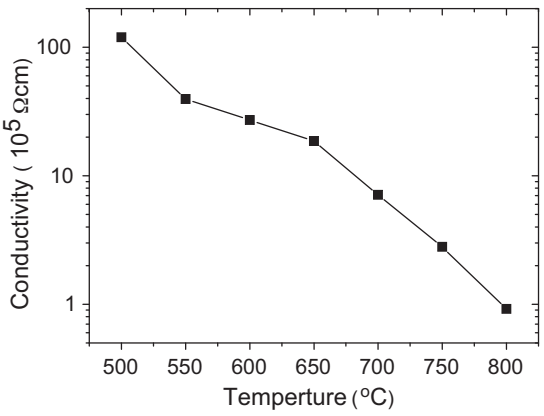

Fig. 5. The electrical conductivity as a function of temperature for the YBA glass.

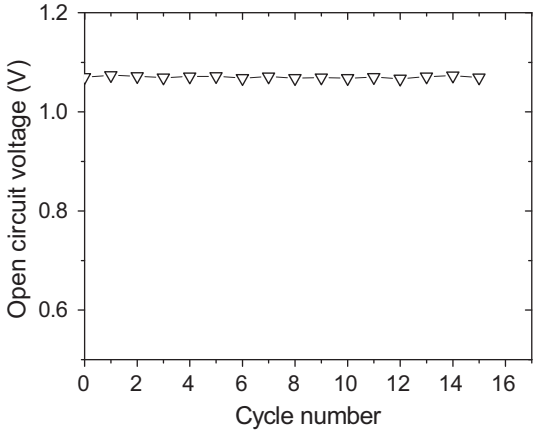

Fig. 6. Changes of the open circuit voltages for the YBA glass after thermal cycles.

where A is a preexponential factor, k is the Boltzmann constant, T is the absolute temperature and E_a is the activation energy for conduction. By fitting the slope of the plot, the activation energy is calculated to be 209 kJ/mol.

The glass sealant is responsible for the gas-tight separation of the air and the fuel gas chambers, air-manifold from the fuel electrode, and H_2-manifold from the air-electrode porosities. The sealing test unit was arranged as an oxygen concentration cell, and the open circuit voltage (OCV, E) is given by the Nernst equation (5):

$$E = \frac{RT}{4F} Ln \frac{P_{O_{2(air)}}}{PO_{2(H_2)}} \quad (5)$$

where R is the gas constant, F is the Faraday constant, and P is the partial pressure of oxygen at the electrodes. Fig. 6 shows the change of OCV of YSZ electrolyte with thermal cycles. The heating and cooling rates of the cycles are 5 °C/min and 3 °C/min, respectively. The OCV values are very close to the theoretical value. The voltage at 750 °C nearly kept stable after 15 cycles, indicating the sealing was effective even after 15 thermal cycles.

4. Conclusions

The YBA glass has been studied as potential SOFC sealant. The resistivity of the YBA glass below 800 °C is over $9.1 \times 10^4\ \Omega$ cm which can fulfill the requirement of SOFCs. The YBA glass has a CTE of $11.64 \times 10^{-6}\ K^{-1}$ near other SOFC components below 873 K and it becomes flexible over that temperature. It was proved that the YBA glass adheres well to YSZ and other SOFC components according to the SEM investigations. Preliminary results demonstrated that the YBA glass appears to be a most promising sealant for planar SOFCs.

Acknowledgments

The authors gratefully thank the financial support from Anhui Key Laboratory of Information Materials and Devices, and National Natural Science Foundation of China (Grant No. 11074001).

References

[1] N.Q. Minh, J. Am. Ceram. Soc. 76 (1993) 563–588.
[2] B.C.H. Steele, A. Heinzel, Nature 414 (2001) 345–352.
[3] S.C. Singhal, Solid State Ionics 152–153 (2003) 405–410.
[4] J.W. Fergus, J. Power Sources 147 (2005) 46–57.
[5] M.K. Mahapatra, K. Lu, Mater. Sci. Eng. R 67 (2010) 65–85.
[6] Y.S. Chou, J.W. Stevenson, J. Power Sources 112 (2002) 376.
[7] F. Wiener, M. Bram, H.P. Buchkremer, J. Mater. Sci. 42 (2007) 264.
[8] S. Sang, W. Li, J. Pu, L. Jian, J. Power Sources 177 (2008) 77.
[9] J. Duquette, A. Petric, J. Power Sources 137 (2004) 71.
[10] S.P. Simner, J.W. Stevenson, J. Power Sources 102 (2001) 310.
[11] S.J. Widgeon, R.E. Loehman, et al., J. Am. Ceram. Soc. 92 (2009) 781.
[12] F. Smeacetto, M. Salvo, P. Asinari, et al., J. Eur. Ceram. Soc. 28 (2008) 611.
[13] M.K. Mahapatra, K. Lu, R.J. Bodnar, Appl. Phys. A 95 (2009) 49.
[14] S. Ghosh, R.N. Basu, H.S. Maiti, et al., J. Eur. Ceram. Soc. 28 (2008) 69.
[15] Y.S. Chou, J.W. Stevenson, P. Singh, J. Power Sources 185 (2008) 1001.
[16] C. Story, K. Lu, W.T. Reynolds Jr., D. Brown, Int. J. Hydrogen Energy 33 (2007) 3970.
[17] H. Shao, T. Wang, Q. Zhang, J. Alloy Compd. 484 (2009) 2–5.
[18] S. Le, N. Zhang, Y. Mao, et al., J. Alloy Compd. 496 (2010) 96–99.
[19] F. Smeacetto, M. Ferraris, et al., J. Eur. Ceram. Soc. 30 (2010) 933–940.
[20] J. Cheng, D. Xiong, H. Li, H. Wang, J. Alloy Compd. 507 (2010) 531–534.
[21] R. Wang, Z. Lü, C. Liu, et al., J. Alloy Compd. 432 (2007) 189–193.
[22] F. Smeacetto, M. Ferraris, et al., J. Power Sources 190 (2009) 402–407.
[23] T. Sun, H. Xiao, W. Guo, X. Hong, Ceram. Int. 36 (2010) 821–826.
[24] R. Zheng, S.R. Wang, H.W. Nie, T.L. Wen, J. Power Sources 128 (2004) 165–172.
[25] S. Ghosh, A. Das Sharma, R.N. Basu, et al., Int. J. Hydrogen Energy 35 (2010) 272–283.
[26] N. Laorodphan, T. Chairuangsri, et al., J. Non-Cryst. Solids 355 (2009) 38–44.
[27] A. Goel, M.J. Pascual, J.M.F. Ferreira, Int. J. Hydrogen Energy 35 (2010) 6911–6923.
[28] S. Sakka, J.D. Mackenzie, J. Non-Cryst. Solids 6 (1971) 145.
[29] G.S. Fulcher, J. Am. Ceram. Soc. 8 (1925) 399.